

Uniaxial Commensurate-Incommensurate Transition in Surface Films: Xe Adsorbed on Cu(110)

M. Jaubert, A. Glachant, M. Bienfait, and G. Boato^(a)

Département de Physique,^(b) Faculté des Sciences de Luminy, Université d'Aix-Marseille II, F-13288 Marseille, France

(Received 18 February 1981)

Low-energy-electron-diffraction and Auger-electron-spectroscopy measurements indicate the existence of an uniaxial commensurate-incommensurate transition in a solid monolayer of xenon adsorbed on the (110) face of copper. The critical exponent describing the variation of the lattice constant versus chemical potential is consistent with the value $\frac{1}{2}$ predicted by Pokrovsky and Talapov.

PACS numbers: 68.20.+t, 64.60.Fr

The commensurate-incommensurate transition ($C-I$) in surface films is the subject of intensive research.¹⁻⁶ A recent theory by Pokrovsky and Talapov⁷ predicts that a solid monolayer adsorbed on an anisotropic crystalline surface can undergo an uniaxial commensurate-incommensurate ($C-I$) transition whose critical behavior is given by

$$\Delta d = C(\Delta\mu)^{1/2}, \quad (1)$$

where Δd and $\Delta\mu$ are, respectively, the variation, at the transition, of the overlayer lattice and the chemical potential. C is a proportionality constant. This work raised considerable interest among theoreticians and several of them revisited the uniaxial $C-I$ transition with slightly different models.⁸⁻¹¹ They all deduced a critical exponent $\frac{1}{2}$ [Eq. (1)] in the vicinity of the transition.

We present here what we believe to be the first measurement of the critical exponent of an uniaxial $C-I$ transition in surface films. Our experiment was performed on a xenon monolayer adsorbed on the (110) face of copper. We show that the adsorbed layer undergoes an uniaxial compression upon increasing the chemical potential and that the variation of the lattice constant obeys Eq. (1) within the experimental uncertainty. Furthermore, we are able to estimate the value of C .

The (110) face of copper exhibits parallel troughs in the $[1\bar{1}0]$ direction (Fig. 1). They favor the condensation of xenon atoms as shown in a preliminary low-energy-electron-diffraction (LEED) study by Chesters, Hussain, and Pritchard.¹² The solid-layer formation begins with a commensurate $c(2 \times 2)$ structure which is readily converted into an incommensurate film upon further chemical-potential increase. The compression occurring in the $[1\bar{1}0]$ direction only, as indicated in Fig. 1, provides us with a good physical realization of an uniaxial $C-I$ phase transition.

We thoroughly analyzed this transition by low-

energy electron diffraction (LEED) and Auger-electron spectroscopy (AES) at 75, 77, and 79 K. The copper (110) surfaces were obtained by cutting ~1-mm slices from an oriented single-crystal rod (99.999% purity) by spark erosion. After chemical polishing, the crystal was cleaned by repeated cycles of argon-ion bombardment and annealing at 500 °C until a very sharp LEED pattern developed and the Auger spectrum exhibited no impurities (except for slight traces of carbon that were impossible to remove).

The xenon condensation was monitored by recording the 40-eV Xe $N_{4.5}O_{2.3}O_{2.3}$ Auger peak as a function of the equilibrium xenon pressure p at constant temperature (adsorption isotherm). The Auger peak-to-peak height is proportional to

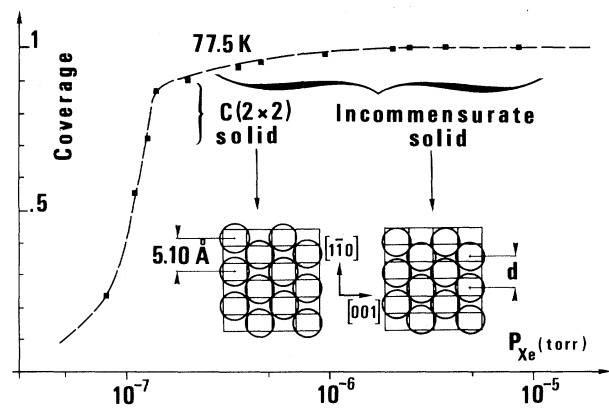


FIG. 1. An adsorption isotherm measured by Auger-electron spectroscopy (incident energy 1500 eV, target current 1.5 μ A, rms modulation voltage 0.7 V). A gas-commensurate-solid transition is followed by a commensurate-incommensurate ($C-I$) structural change. The $c(2 \times 2)$ and incommensurate-solid domains are identified from the LEED pattern. The inset gives a schematic representation of the $C-I$ transition. An uniaxial compression of the layer occurs along $[1\bar{1}0]$ with increasing pressure.

xenon concentration.¹³ A typical adsorption isotherm is drawn in Fig. 1. Each point represents the equilibrium concentration of the surface film for a given pressure of xenon vapor. A large step is observed in Fig. 1. It corresponds to a gas-solid transition. Above a coverage of 0.9, the concentration of the layer increases gradually by about 10% within one order-of-magnitude pressure range, then stays constant over another order-of-magnitude pressure range. This latter plateau corresponds to monolayer completion (coverage 1).

The formation of the solid is also detected by LEED. A $c(2 \times 2)$ structure first appears and is stable in a narrow domain of pressure. Then the $c(2 \times 2)$ superstructure spots split into doublets featuring the incommensurate solid. A schematic LEED pattern of the out-of-registry structure is represented in the inset of Fig. 2. The spot called a corresponds to the normal reciprocal superlattice whereas the b spot is due to double diffrac-

tion [the b spot disappears for the electron energies where the (10) and (11) substrate peaks are weak]. The distance between a and b varies when the xenon pressure is changed. The incommensurability along the $[1\bar{1}0]$ direction can be determined by measuring the distances between two superstructure peaks (a and b) and between two substrate peaks (A and B). The lattice constant of the $[1\bar{1}0]$ copper row being 2.55 \AA , it is straightforward to show that the mean distance d between Xe atoms along the troughs (in angstroms) is $5.10AB/(AB+ab)$. Numerous LEED pictures have been taken at constant temperature for different xenon pressures. Temperature is regulated to better than $\pm 0.2 \text{ K}$. The pressure fluctuations during the picture recording are indicated by the bars in Fig. 2 (absolute values are known to within $\pm 1 \text{ K}$ and a factor of 2 in pressure).

Positions and shapes of the diffracted beams were measured with a microdensitometer. They yield the variation of d with p . A typical result is plotted in Fig. 2 for 77 K . The mean distance between xenon atoms along the $[1\bar{1}0]$ canals continuously varies from $d_0 = 5.10 \text{ \AA}$ [commensurate $c(2 \times 2)$ structure] to $4.62 \pm 0.02 \text{ \AA}$ (completion of the incommensurate solid). At this point, it is worth recalling that the distance between xenon $[1\bar{1}0]$ rows stays unchanged (3.605 \AA). The nearest-neighbor distance at completion of the monolayer is 4.28 \AA , close to the 4.26 \AA observed for xenon on graphite in Ref. 3. In Fig. 2, there are no experimental points between 4.9 and 5.1 \AA . Very close to the transition, the two superstructure peaks due to the incommensurate solid overlap and become broader than in the C and I phases. The spot widths in the various regimes are $\Delta k \approx 0.16 \text{ \AA}^{-1}$ for the C and I solids and $\Delta k \sim 0.25 \text{ \AA}^{-1}$ near the transition where the broadening is observed. The instrumental resolution determined from the sharpness of the Cu peaks is $\Delta k = 2\pi \Delta\theta/\lambda = 0.09 \text{ \AA}^{-1}$, where $\Delta\theta$ is the full width at half maximum of the spots. The broadening is consistent with the phenomena of metastability of the periodic distortions close to the transition predicted a long time ago by Frank and van der Merwe.¹⁴ This could also be due to a fluid phase which is expected to be stable between the commensurate and incommensurate solid.¹⁵ For this domain, it is experimentally difficult to define a lattice constant d .

The uniaxial compression is tested in Fig. 3 against the Pokrovsky-Talapov theory for 75 , 77 , and 79 K . $\Delta d = d_0 - d$ represents the variation of the mean xenon lattice constant and $\Delta\mu = kT \ln(p/$

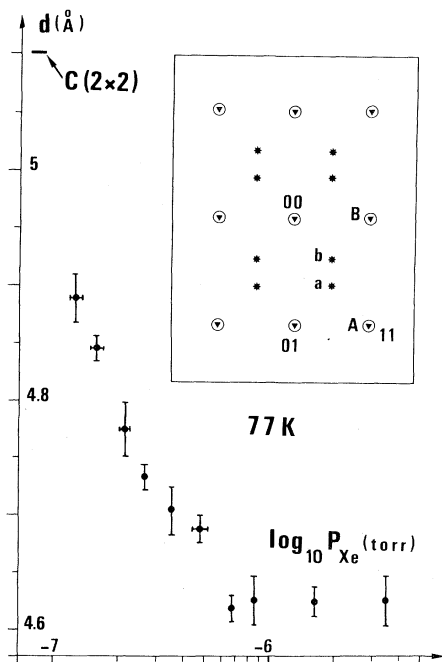


FIG. 2. The mean distance between Xe atoms varies continuously at the C - I transition. The lattice constant d along the $[1\bar{1}0]$ direction of compression is obtained from LEED patterns similar to that idealized in the box; it is determined by relative measurements of ab and AB . Parameters for the normal incidence electron beam were 146 eV and $2.5 \mu\text{A}$. In all the AES and LEED measurements, the intensity of the incident beam was reduced so that no electron-stimulated desorption was detected. Inset: The triangles within circles are copper spots; the asterisks are xenon superstructure spots.

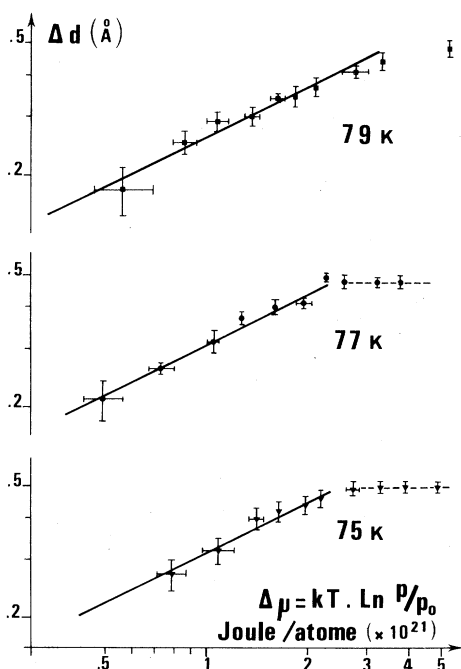


FIG. 3. Variation of the lattice constant along the direction of the uniaxial $C-I$ transition vs the corresponding variation of the chemical potential, in a log-log scale. Our results are consistent with the value $\frac{1}{2}$ of the critical exponent for the three temperatures analyzed [the solid lines are the prediction of Eq. (1)]. The dotted lines correspond to the saturation of the incommensurate structure. $p_0 = 1.7 \times 10^{-7}$, 8×10^{-8} , and 3.6×10^{-8} Torr for 79, 77, and 75 K, respectively.

p_0) is the variation of the chemical potential at the $C-I$ transition. The pressure p_0 is defined by the appearance of the broadening of the $c(2 \times 2)$ superstructure spots on the LEED pattern. It corresponds to a coverage of about 0.9 in the adsorption isotherm measurements (see Fig. 1). p_0 is known to within $\pm 10\%$. One must point out that there are no adjustable parameters in this representation. The full lines in the $\log \Delta d$ vs $\log \Delta \mu$ diagram represent Eq. (1). Their slope is $\frac{1}{2}$, the value of the critical exponent predicted by the theory. It can be seen that the experimental data are consistent with the theory of Pokrovsky and Talapov all along the uniaxial transition.¹⁶ The dotted lines represent the saturation of the incommensurate layer.

We also checked that our results do not satisfy the $T=0$ result based on the theory of Frank and Van der Merwe ($|\Delta d| \sim |\ln \Delta \mu|^{-1}$).^{4, 14}

Finally, we calculated the proportionality factor C from the experimental data in Fig. 3. Its mean

value for the three sets of data in Fig. 3 is $0.9 \pm 0.1 \text{ mJ}^{-1/2} \text{ atom}^{-1/2}$. The large uncertainty is due to the inaccuracy in the determination of p_0 .

The authors wish to thank U. Bardi for the preparation of the copper sample, J. Villain for valuable discussions and correspondence, and J. Friedel for helpful comments.

^(a)Permanent address: Istituto di Scienze Fisiche and Gruppo Nazionale de Struttura della Materia—Consiglio Nazionale delle Ricerche, Università di Genova, I-16126 Genova, Italy.

^(b)Member of Equipe de recherche associée au Centre National de la Recherche Scientifique.

¹M. D. Chinn and S. C. Fain, Phys. Rev. Lett. **39**, 146 (1977); S. C. Fain, M. D. Chinn, and R. D. Diehl, Phys. Rev. B **21**, 4170 (1980).

²P. W. Stephens, P. Heiney, R. J. Birgeneau, and P. M. Horn, Phys. Rev. Lett. **43**, 47 (1979); R. J. Birgeneau, E. M. Hammons, P. Heiney, P. W. Stephens, and P. M. Horn, in *Ordering in Two Dimensions*, edited by S. K. Sinha (North-Holland, New York, 1980), p. 29.

³J. S. Venables and P. S. Schabes-Retchkiman, J. Phys. (Paris), Colloq. **38**, C4-105 (1977), and to be published.

⁴J. Villain, in *Ordering in Strongly Fluctuating Systems*, edited by T. Riste (Plenum, New York, 1980), p. 214.

⁵J. Villain, Surf. Sci. **97**, 219 (1980).

⁶*Phase Transitions in Surface Films*, edited by J. G. Dash and J. Ruvalds (Plenum, New York, 1980).

⁷V. L. Pokrovsky and A. L. Talapov, Phys. Rev. Lett. **42**, 65 (1979).

⁸H. J. Schulz, Phys. Rev. B **22**, 1 (1980).

⁹T. Nattermann, J. Phys. (Paris) **41**, 1251 (1980).

¹⁰Y. Okwamoto, J. Phys. Soc. Jpn. **49**, 8 (1980).

¹¹M. B. Gordon and J. Villain, J. Phys. C **12**, L151 (1979).

¹²M. A. Chesters, M. Hussain, and J. Pritchard, Surf. Sci. **35**, 161 (1973).

¹³J. Suzanne, J. P. Coulomb, and M. Bienfait, Surf. Sci. **44**, 141 (1974).

¹⁴F. C. Frank and J. H. van der Merwe, Proc. Roy. Soc. London **198**, 205 (1949).

¹⁵S. N. Coppersmith, D. S. Fisher, B. I. Halperin, P. A. Lee, and W. F. Brinkman, Phys. Rev. Lett. **46**, 549 (1981).

¹⁶Two kinds of analysis of our most precise data (77 K) have been carried out. A straight-line fit with no adjustable parameter yields a slope 0.54 with a reliability factor $r^2 = 0.9902$ and a standard deviation $s_1 = 0.024$. By letting both the slope and p_0 be adjustable parameters, the best straight line has a slope 0.51, $r^2 = 0.9903$, and $s_1 = 0.022$ (then the best p_0 is 8.5×10^{-8} Torr).